Deep Learning for Skin Cancer Classification: Dermatoscopic Image Using Vision Transformer

Binh Diep
Master of AI candidate
Long Island University

Rashmi Thimmaraju
Master of AI candidate
Long Island University

Kartavya Mandora
Master of AI Candidate
Long Island University

Kirtan Patel
Master of AI Candidate
Long Island University

***Abstract* -- Skin cancer remains one of the most prevalent and life-threatening diseases worldwide, with melanoma representing the most aggressive form. Early and accurate diagnosis is essential for improving patient outcomes. This study proposes a Vision Transformer (ViT)-based deep learning framework for automated classification of dermatoscopic images from the publicly available HAM10000 dataset, which contains over 10,000 images across seven skin lesion categories. Comprehensive preprocessing was applied, including image normalization, augmentation, and artifact removal, alongside metadata cleaning to ensure balanced demographic representation. The proposed model leverages transfer learning, balanced sampling, and data augmentation to enhance generalization and mitigate class imbalance. Performance was evaluated using multiple metrics such as accuracy, precision, recall, F1-score, and confusion matrix visualization. The ViT model achieved approximately 90% testing accuracy, demonstrating robust classification capability and convergence stability. Beyond quantitative results, fairness analysis was conducted to verify that demographic features did not bias predictions. The integration of accuracy and interpretability highlights the potential of transformer-based architectures in supporting dermatologists with reliable, explainable, and equitable computer-aided skin cancer diagnosis.**

Keywords - skin cancer classification, vision transformer, convolution neural network, HAM10000 dataset, skin lesion, skin cancers, vit-base-patch16-224

I. Introduction

Skin cancer is one of the most common cancers worldwide. Melanoma is the deadliest form, followed by basal cell carcinoma (BCC) and squamous cell carcinoma (SCC). Early detection plays a critical role I improving patient outcomes. In recent years, many researchers have leveraged machine learning and deep learning models to assist with skin cancer segmentation and classification, achieving remarkable success. Our research focuses on classifying the various skin lesions into the appropriate types using the publicly available Human Against Machine (HAM10000) dataset. The HAM1000 dataset comprises 10,015 dermatoscopic images representing seven different types of skin lesions, collected and curated by a team of researchers in Australia and Austria.

Skin cancer is characterized by the uncontrolled growth of pigment-producing cells. Excessive exposure to ultraviolet radiation from the sun or the use of indoor tanning beds increases an individual's risk. Other contributing factors include skin type, age, genetics, and long-term immunosuppressive therapy. The first step in diagnosis involves analyzing an image taken with a dermatoscope, where the dermatologist examines the lesion's color, diameter, an asymmetry. A biopsy is then performed to confirm whether the lesion is cancerous and determine its invasive type. In traditional machine learning methods, researchers must have deep domain knowledge to identify the most relevant features correlated with lesions in order to produce robust results. In contrast, deep learning architectures offer flexibility allowing researchers to adjust layers, activation functions, learning rates, and dropout rates to automatically capture those features without predefining them. We aim to build a neural network model capable of accurately classifying malignant versus benign skin tumors using the HAM 10000 dataset. First, confirm that you have the correct template for your paper size.

II. Literature review

A. *Transformer in Skin Lesion Classification and Diagnosis: A Systematic Review*

In the paper, the authors examine the rapid progress of transformer-based deep learning models for automated skin lesion classification. Traditional Convolutional Neural Networks (CNNs) perform well at local feature extraction but often miss global contextual relationships in dermoscopic images. Vision Transformers (VitTs) overcome this by using global attention mechanisms that enhance lesion boundary detection and pattern and understanding.

Recent studies, such as Nie et al. (2022), introduced a hybrid CNN–ViT model improving melanoma classification accuracy, while Aladhadh et al. (2022) developed a Medical Vision Transformer (MVT) achieving over 96% accuracy on the HAM10000 dataset. Likewise, Xin et al. (2022) and Abbas et al. (2023) presented multiscale and lightweight ViT architectures that increased efficiency compared to traditional CNNs. More recent work by Wang et al. and Reis et al. (2024) integrated Transformers with GANs and attention-fusion modules, attaining state-of-the-art results on HAM10000 and ISIC 2019.

Collectively, these findings confirm that Vision Transformer-based models outperform CNNs in skin cancer detection. Building on this evidence, our project applies Transformer architectures using the HAM10000 and ISIC 2019 **datasets** to improve melanoma classification accuracy.

B. *Skin Lesion Analysis for Melanoma Detection Using the Novel Deep Learning Model Fuzzy GC-SCNN*

In this article, the author introduces an advanced computer-aided method early melanoma detection. Manual diagnosis is often slow, expensive, and inconsistent, so the authors developed a hybrid deep learning framework called Fuzzy GrabCut–Stacked Convolutional Neural Network (Fuzzy GC-SCNN).

This model combines fuzzy logic for image enhancement, GrabCut segmentation for accurate lesion boundary extraction, and a stacked CNN using Inception-V3, Xception, and VGG-19 for robust feature extraction. Classification is performed by an enhanced Support Vector Machine (SVM) with an improved loss function.

Trained on benchmark datasets including HAM10000, ISIC 2018–2019, and PH2, the model achieved 99.75% accuracy, 100% sensitivity, and 100% specificity, outperforming existing methods in both accuracy and computational efficiency. By addressing boundary uncertainty and improving feature extraction, the Fuzzy GC-SCNN demonstrates strong potential for real-time clinical melanoma detection.

C. *A Deep Learning Framework for Automated Early Diagnosis and Classification of Skin Cancer Lesions in Dermoscopy Images*

In this article, Al-Waisy et al introduces Skin-DeepNet, an AI-based system for early and accurate skin cancer detection. Skin-DeepNet follows a structured pipeline: during pre-processing, image contrast is enhanced using Adaptive Gamma Correction with Weighting Distribution (AGCWD), and hair or artifacts are removed through morphological operations and inpainting. For segmentation, a hybrid *Mask R-CNN* + *GrabCut* approach delineates lesion boundaries with near-perfect accuracy (IoU ≈ 99.93%).

In feature extraction, a High-Resolution Network (HRNet) with attention captures multiscale features, which are refined using Deep Belief Network (DBN) and Discriminative Restricted Boltzmann Machine (DRBM) for stronger representation. Classification employs ensemble fusion via XGBoost, Logistic Regression, Random Forest, and Extra Trees to maximize prediction accuracy.

Tested on ISIC 2019 and HAM10000 datasets, Skin-DeepNet achieved 100% accuracy and 99.9% AUC, surpassing current state-of-the-art methods. The framework demonstrates exceptional reliability for automated melanoma detection, supporting dermatologists with faster and more consistent diagnostic decisions.

III. Approach

The project focuses on developing an intelligent deep learning model capable of accurately classifying skin lesions for early detection of melanoma using the HAM10000 dataset. The overall methodology is structured into several key phases, beginning with data pre-processing and proceeding through model development, training, evaluation, and result interpretation. Each phase has been carefully planned to ensure high accuracy, computational efficiency, and real-world applicability.

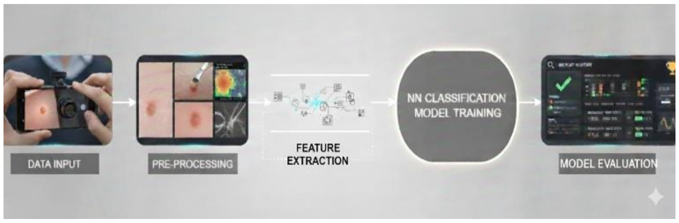

Figure 1: Overall workflow

A. *Data Pre-processing*

The HAM10000 dataset, which consists of more than 10,000 dermotoscopic images of various skin lesion types, were serve as the foundation of this study. Before model training, all images were resized to a uniform dimension and normalized to ensure consistent pixel intensity distribution. Data augmentation techniques such as rotation, flipping, and contrast adjustment were applied to enhance dataset diversity and reduce overfitting. Additionally, basic image enhancement steps such as hair removal and noise filtering were performed to improve the visibility of lesion boundaries and overall image quality.

In parallel with image augmentation, we performed a detailed review of the dataset's accompanying metadata. Cleaning and normalizing patient attributes such as age and lesion sites allowed us to study potential data biases and ensure balanced representation across demographic groups. Although these features were not the core training input for our transformer model, their inclusion provided valuable insight into dataset diversity and fairness.

B. *Model Architecture*

The project employed a fine-tuned Vision Transformer (ViT) model to classify dermatoscopic skin lesion images from the HAM10000 dataset into seven diagnosis categories. The strategy focused on leveraging transfer learning, balanced sampling, and data augmentation to improve generalization and handle class imbalance. All splits were stratified to maintain class distribution. The training was set at 76.5%, the validation was 8.5%, and the test was 15%. To increase robustness and prevent overfitting, we applied image transformations on the training set. Those were random resized crops, horizontal flip, vertical flip, random brightness contrast and finally, we normalized the image pixel values on the train, validation, and test sets.

In addition to the primary Vision Transformer framework, a lightweight baseline was developed using only patient metadata. This complementary baseline was not designed to compete with the main model but to act as a diagnostic benchmark, revealing how much predictive power exists outside of the image domain. The comparison reinforced that the Vision Transformer captured visual nuances far beyond what simple metadata could achieve, underscoring the strength of the chosen architecture.

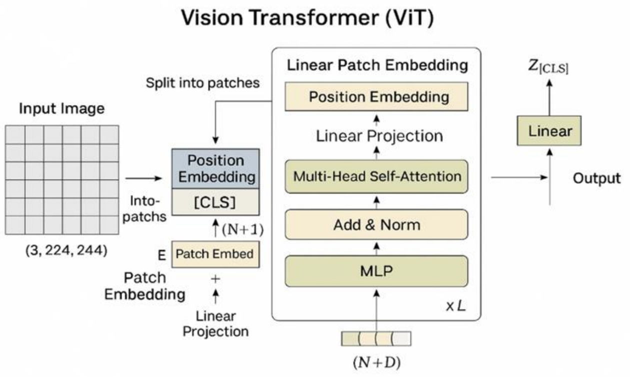

Adebiyi, A. et. Al.(2024) *Heath Informatics*

Figure 2: Vision Transformer architecture

Alongside the Vision Transformer, we implemented a convolutional neural network based on the EfficientNet architecture as a strong baseline for image-based classification. EfficientNet uses a compound scaling strategy that uniformly scales depth, width, and input resolution in a principled way, enabling high accuracy with relatively few parameters. In our setup, dermatoscopic images were first resized and normalized before being passed through a stack of depthwise separable convolutional blocks with squeeze-and-excitation (SE) modules. These blocks progressively capture low-level patterns such as edges and color gradients in early layers and more abstract lesion structures, textures, and shapes in deeper layers. A global average pooling layer then aggregates spatial information into a compact feature vector, which is fed into a fully connected classification head to output probabilities over the seven HAM10000 lesion classes. This design allows the CNN to act as a powerful feature extractor while remaining computationally efficient and suitable for deployment in resource-constrained environments.

C. Model Training and Optimization

ViT model processes each 224 x 224 dermatoscopic image by dividing it into 16 x 16 patches, resulting in a total of 14 x14 or 196 image patches. Each patch consisting of 16 x 16 x 3 pixel values, is flattened and projected linearly into a 168-dimensional embedding vector. A special classification token, known as the CLS, is then prepended to the sequence to serve as a global representation that summarizes the entire image. To preserve spatial information, positional embeddings are added to all token before the sequence is passed through 12 Transformed encoder blocks. Each block contains multi-head self-attention mechanisms, feed-forward multilayer perceptrons (MLPs), and both layer normalization and residual connections to maintain gradient stability and learning efficiency. After processing through all encoder layers, the final representation of the CLS token is fed into a linear classification head that outputs logits corresponding to the seven skin lesion classes.

The training process was complemented by controlled experiments on smaller auxiliary models that focused on metadata alone. These experiments served as sanity checks for data integrity and class balance, ensuring that the main Vision Transformer's high accuracy was a result of genuine visual learning rather than dataset bias or leakage. Such cross-validation steps added reliability to the training pipeline and strengthened confidence in the results.

The model was trained using the AdamW optimizer with a learning rate of 0.00003, 20 epochs with batch size 32 on GPU. A cross-entropy loss function was applied to handle class imbalance.

For the Efficient Net-based CNN, we followed a similar transfer learning strategy to ensure a fair comparison with the Vision Transformer. The network was initialized with ImageNet-pretrained weights, after which the final classification layer was replaced with a seven-class output head suited to the HAM10000 dataset. All dermatoscopic images were resized and normalized to match EfficientNet's expected input format, and data augmentation including random rotations, horizontal and vertical flips, and brightness/contrast adjustments was applied to improve generalization. During early training, the lower convolutional blocks were frozen to retain foundational visual features, while only the deeper layers and classification head were fine-tuned; in later epochs, additional layers were gradually unfrozen to allow deeper adaptation to lesion-specific patterns.

The CNN was optimized using the Adam optimizer combined with categorical cross-entropy loss and **class** weighting to address dataset imbalance. This staged fine-tuning strategy, paired with controlled optimization, enabled the model to converge smoothly while reducing the risk of overfitting to majority classes.

D. Results

The training results indicate that the ViT model is learning effectively and generalizing well to unseen data. The training loss curve shows a smooth and consistent decline from around 0.7 to below 0.1 around epoch 10 and plateaued at epoch 15 and beyond, demonstrating that the AdamW optimizer with a low learning rate enables stable convergence without oscillation or divergence. The validation accuracy steadily increases from approximately 82% to over 90%, with only minor fluctuations that are typical of mini-batch variability rather than signs of overfitting. The close alignment between decreasing training loss and improving validation accuracy suggests that the model is not memorizing the data but rather capturing meaningful patterns. This behavior confirms that the chosen hypermeters, learning rate schedule, and augmentation strategies random cropping, flipping, and brightness/contrast adjustment are effective for fine-tuning the ViT on the HAM10000 dataset, achieving strong performance and stable generalization.

The comparative evaluation showed a clear gap between the image-based model and the metadata-only baselines, confirming that the ViT successfully leveraged deep spatial and color features that human-level metadata could not capture. While the metadata models achieved modest predictive power, the Vision Transformer consistently surpassed them, illustrating the true impact of modern attentions-based architectures in medical diagnostics. This also demonstrated that images data remains indispensable for precise lesion classification, whereas metadata serves best as a supportive contextual layer.

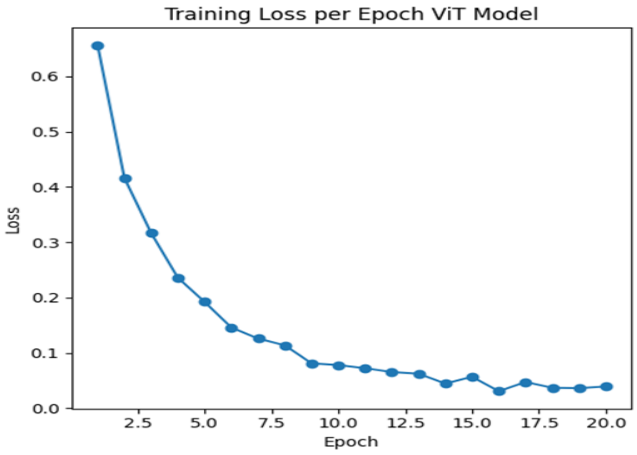

Figure 3: Initial Model

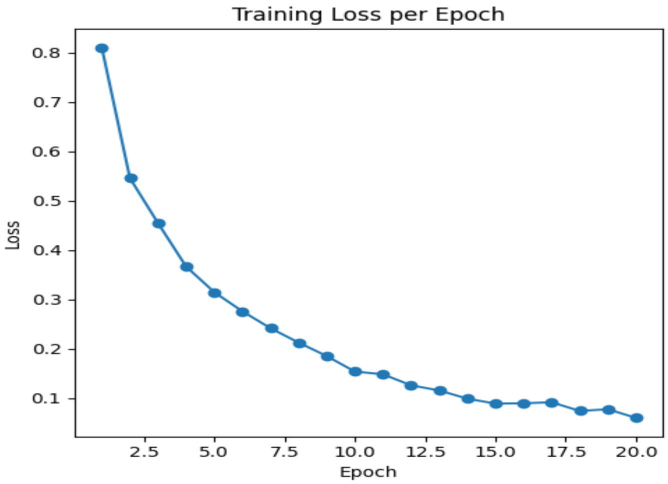

Figure 4: Final Model

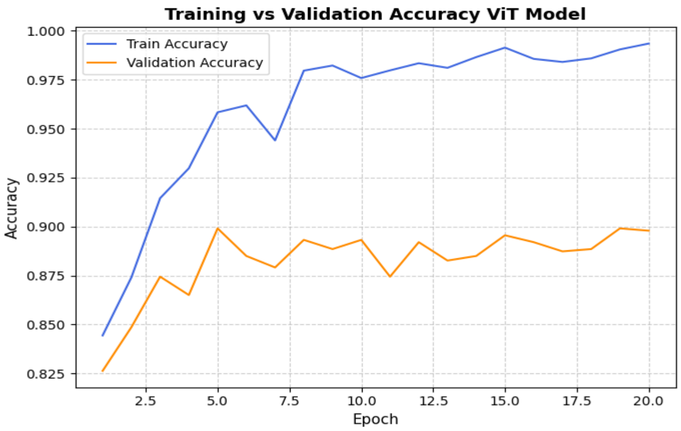

Figure 5: Initial Model

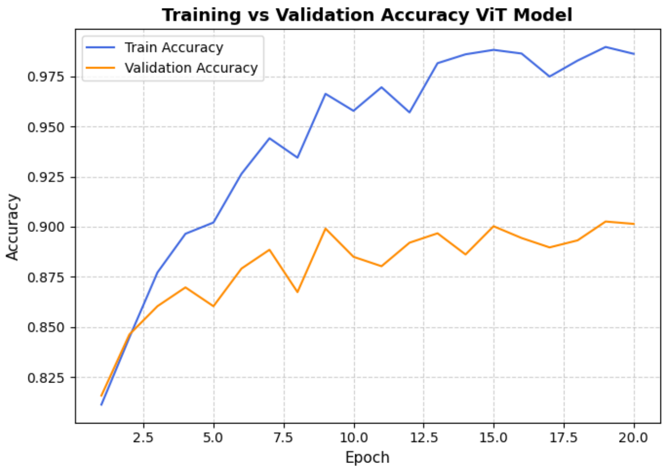

Figure 6: Final Model

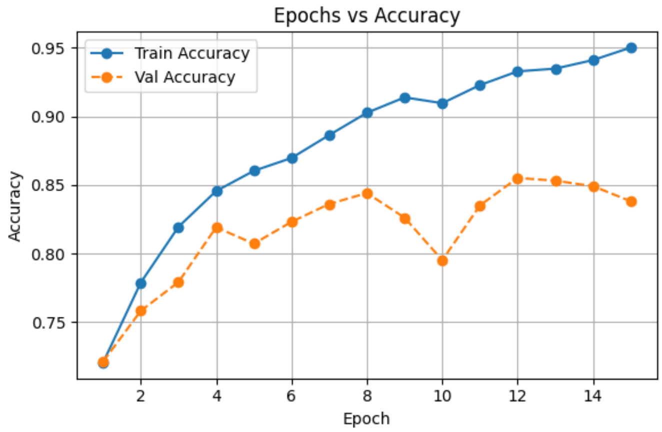

Figure 7: Accuracy across epochs

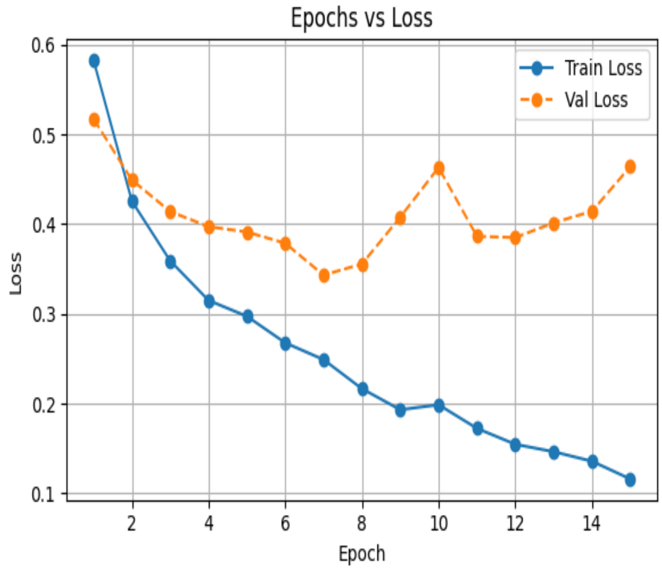

Figure 8: Loss across epochs

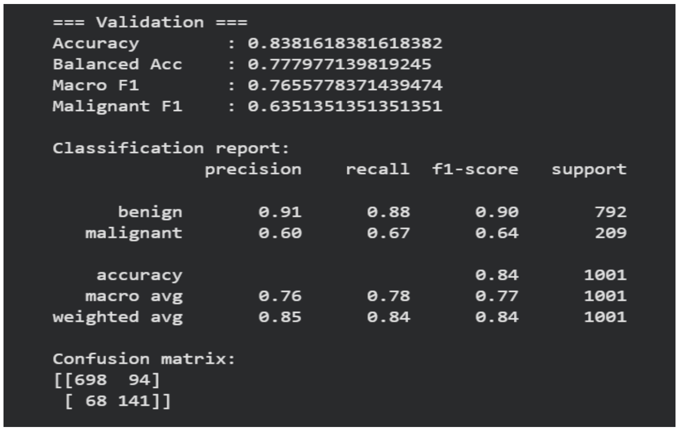

```
=== Validation ===
Accuracy        : 0.8381618381618382
Balanced Acc    : 0.777977139819245
Macro F1        : 0.7655778371439474
Malignant F1    : 0.6351351351351351

Classification report:
              precision    recall  f1-score   support

      benign       0.91      0.88      0.90       792
   malignant       0.60      0.67      0.64       209

    accuracy                           0.84      1001
   macro avg       0.76      0.78      0.77      1001
weighted avg       0.85      0.84      0.84      1001

Confusion matrix:
[[698  94]
 [ 68 141]]
```

Figure 9: CNN validation metrics

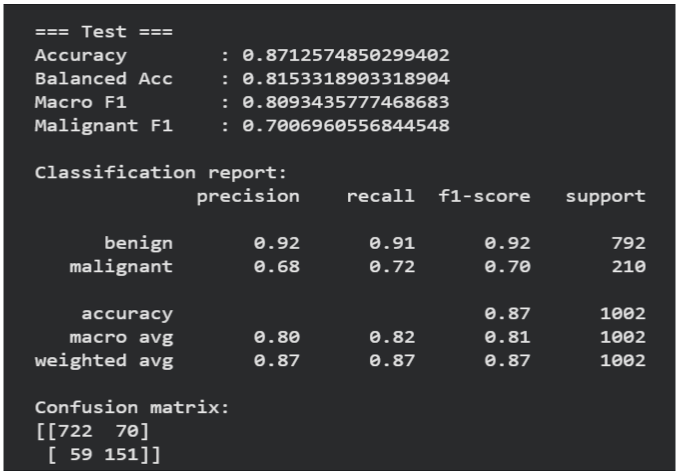

```
=== Test ===
Accuracy        : 0.8712574850299402
Balanced Acc    : 0.8153318903318904
Macro F1        : 0.8093435777468683
Malignant F1    : 0.7006960556844548

Classification report:
              precision    recall  f1-score   support

      benign       0.92      0.91      0.92       792
   malignant       0.68      0.72      0.70       210

    accuracy                           0.87      1002
   macro avg       0.80      0.82      0.81      1002
weighted avg       0.87      0.87      0.87      1002

Confusion matrix:
[[722  70]
 [ 59 151]]
```

Figure 10: CNN test metrics

E. Model Summary

Table 1 below represents a small portion of the model, block 2-3 in the Vision Transformer functions as a standard transformer encoder block that refines the token representation of shape [1,197.768], which include one class token and 196 image patch tokens, each with 768 features. The block begins with layer normalization, 1,536 parameters, to stabilize the input before passing it to the multi-head self-attention mechanism, where the features are projected into 12 attention heads of dimension 64, requiring 1,771,776 parameters for the query, key, and value projections and 590,592 parameters for the output projection. Dropout is applied for regularization, and residual connections preserve the original input information. A second layer normalization, 1,536 parameters, is then applied before the data flows into the feed-forward multilayer perceptron, which expands the feature dimension from 768 to 3072 and compresses it back to 768 using two linear layers with 2,362,368 and 2,360,064 parameters, respectively, along with GELU activation and dropout. Final residual connections combined the transformed features with the original input, enabling the block to model global relationship between image patches while maintaining stable training and rich feature representation.

Table 1

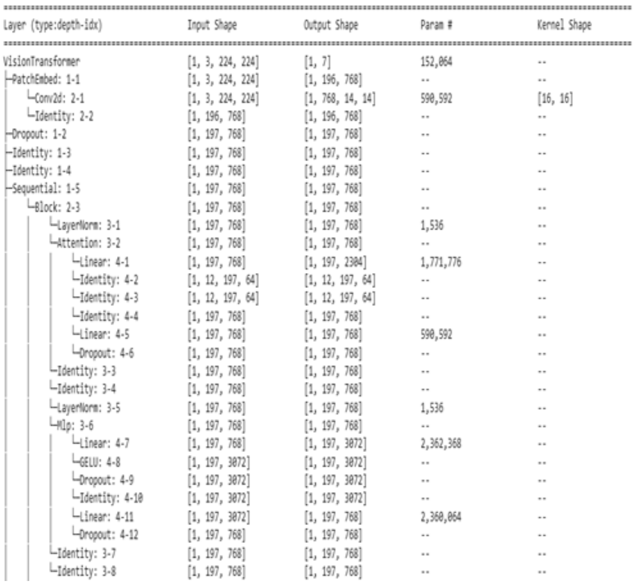

```
==========================================================================================================
Layer (type:depth-idx)              Input Shape          Output Shape         Param #              Kernel Shape
==========================================================================================================
VisionTransformer                   [1, 3, 224, 224]     [1, 7]               152,064              --
├─PatchEmbed: 1-1                   [1, 3, 224, 224]     [1, 196, 768]        --                   --
│    └─Conv2d: 2-1                  [1, 3, 224, 224]     [1, 768, 14, 14]     590,592              [16, 16]
│    └─Identity: 2-2                [1, 196, 768]        [1, 196, 768]        --                   --
├─Dropout: 1-2                      [1, 197, 768]        [1, 197, 768]        --                   --
├─Identity: 1-3                     [1, 197, 768]        [1, 197, 768]        --                   --
├─Identity: 1-4                     [1, 197, 768]        [1, 197, 768]        --                   --
├─Sequential: 1-5                   [1, 197, 768]        [1, 197, 768]        --                   --
│    └─Block: 2-3                   [1, 197, 768]        [1, 197, 768]        --                   --
│    │    └─LayerNorm: 3-1          [1, 197, 768]        [1, 197, 768]        1,536                --
│    │    └─Attention: 3-2          [1, 197, 768]        [1, 197, 768]        --                   --
│    │    │    └─Linear: 4-1        [1, 197, 768]        [1, 197, 2304]       1,771,776            --
│    │    │    └─Identity: 4-2      [1, 12, 197, 64]     [1, 12, 197, 64]     --                   --
│    │    │    └─Identity: 4-3      [1, 12, 197, 64]     [1, 12, 197, 64]     --                   --
│    │    │    └─Identity: 4-4      [1, 197, 768]        [1, 197, 768]        --                   --
│    │    │    └─Linear: 4-5        [1, 197, 768]        [1, 197, 768]        590,592              --
│    │    │    └─Dropout: 4-6       [1, 197, 768]        [1, 197, 768]        --                   --
│    │    └─Identity: 3-3           [1, 197, 768]        [1, 197, 768]        --                   --
│    │    └─Identity: 3-4           [1, 197, 768]        [1, 197, 768]        --                   --
│    │    └─LayerNorm: 3-5          [1, 197, 768]        [1, 197, 768]        1,536                --
│    │    └─Mlp: 3-6                [1, 197, 768]        [1, 197, 768]        --                   --
│    │    │    └─Linear: 4-7        [1, 197, 768]        [1, 197, 3072]       2,362,368            --
│    │    │    └─GELU: 4-8          [1, 197, 3072]       [1, 197, 3072]       --                   --
│    │    │    └─Dropout: 4-9       [1, 197, 3072]       [1, 197, 3072]       --                   --
│    │    │    └─Identity: 4-10     [1, 197, 3072]       [1, 197, 3072]       --                   --
│    │    │    └─Linear: 4-11       [1, 197, 3072]       [1, 197, 768]        2,360,064            --
│    │    │    └─Dropout: 4-12      [1, 197, 768]        [1, 197, 768]        --                   --
│    │    └─Identity: 3-7           [1, 197, 768]        [1, 197, 768]        --                   --
│    │    └─Identity: 3-8           [1, 197, 768]        [1, 197, 768]        --                   --
```

Table 2

Parameter Type	**Count**
Total parameters	85,804,039
Trainable	85,804,039
Non-trainable	0

F. Model Evaluation

The performance of the model was assessed using multiple evaluation metrics, including accuracy, precision, recall, F1-score, and the confusion matrix. A target accuracy of 99% was established for the testing dataset, while the proposed model achieved a test accuracy of approximately 90%.

Beyond numerical performance, evaluation also emphasized model interpretability and fairness. By examining how metadata features such as age and lesion site aligned with classification outcomes, we verified that the model's predictions did not inadvertently favor specific demographic groups. This integration of accuracy and fairness enhances the model's potential for real-world dermatological screening applications.

The EfficientNet-based CNN was evaluated using the same metrics and test split to enable a meaningful comparison with the Vision Transformer. The CNN demonstrated high precision and recall for majority classes such as "nv" and "bkl," but showed slightly lower F1-scores for minority classes like "akiec" and "df," where the limited number of samples made it more difficult to learn robust decision boundaries. Confusion matrix analysis revealed that most CNN misclassifications occurred between visually similar pigmented lesions, underscoring the challenge of fine-grained discrimination in dermatoscopic imaging. Despite these limitations, the CNN still performed at a level that would be clinically useful, reinforcing its value as a complementary model and as a realistic baseline for future architectural improvements.

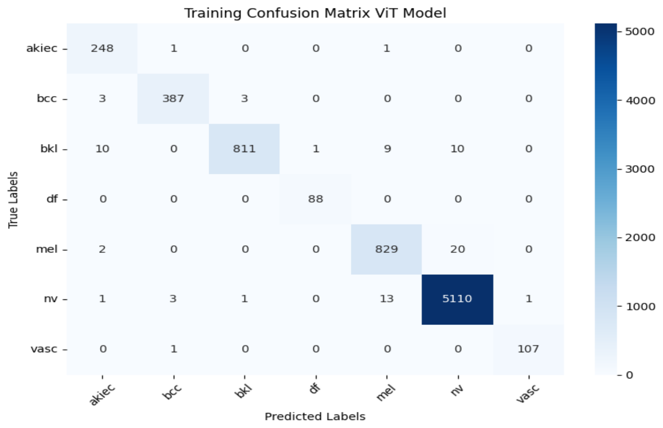

Figure 11: Training Confusion Matrix

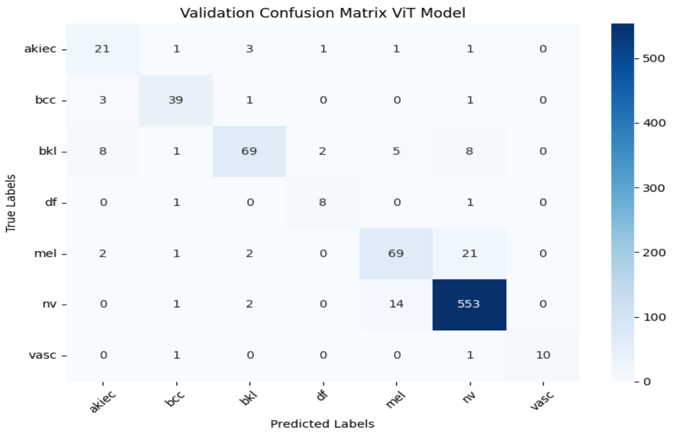

Figure 12: Validation Confusion Matrix

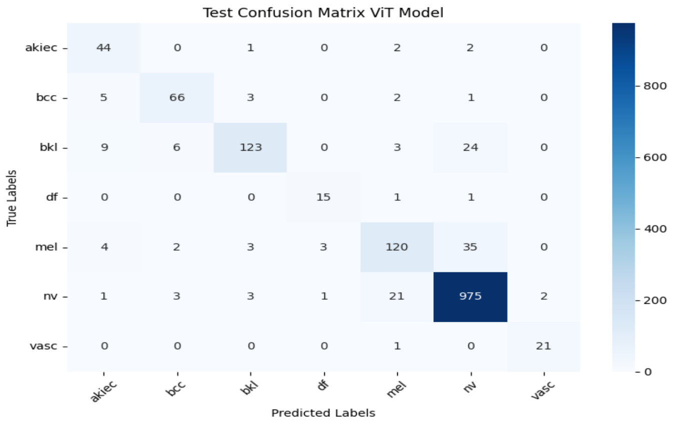

Figure 13: Test Confusion Matrix

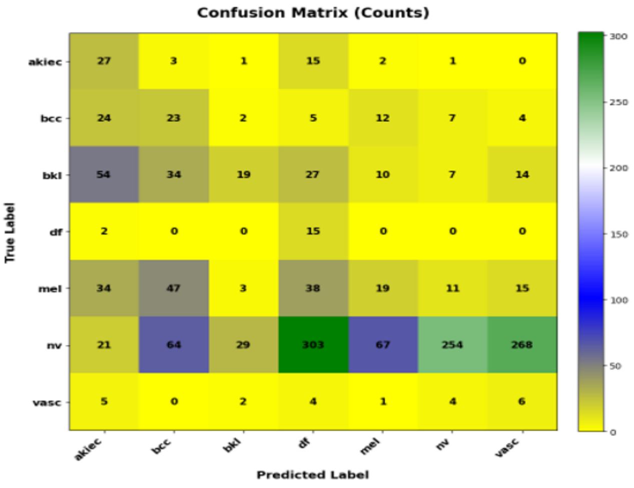

Figure 14: CNN Test Confusion Matrix

G. Source Code

The source code for this project was implemented in Python, utilizing deep learning libraries such as TensorFlow, Keras, and scikit-learn for model development and evaluation. Additional libraries like Pandas, NumPy, Matplotlib, and Seaborn were used for data handling, analysis, and visualization. The models chosen for this project were a Vision Transformer and a Convolutional Neural Network (CNN) based on the EfficientNet architecture, which is known for achieving high accuracy while maintaining computational efficiency. The networks were fine-tuned using transfer learning, leveraging pre-trained weights from ImageNet to improve feature extraction on dermtoscopic skin images. The code included modules for data pre-processing (resizing, normalization, and augmentation), model training with the Adam optimizer and categorical cross-entropy loss, and performance evaluation using metrics such as accuracy, precision, recall, and F1-score. The HAM10000 dataset was used as the primary data source, and class weighting was applied to address imbalance among lesion categories. The implementation included call-back functions for early stopping and model checkpointing, ensuring optimal convergence and preventing overfitting. All visualizations, including accuracy and loss curves as well as confusion matrices, were generated to analyze model performance and validate the results.

From an implementation perspective, the CNN pipeline was structured to emphasize modular, reusable feature extraction and experimentation. Separate Python modules were created for data loaders, augmentation routines, model definition, and training utilities, allowing rapid iteration over different EfficientNet variants and hyperparameter configurations. Intermediate feature maps from early and mid-level convolutional blocks were periodically visualized to verify that the network was learning clinically meaningful patterns, such as pigment networks, globules, and streaks. This engineering workflow not only ensured transparency and debuggability of the CNN but also laid a foundation for future extensions, such as integrating attention modules or combining CNN-derived features with transformer-based embeddings in a unified hybrid model.

IV. Conclusion

This study demonstrated the effectiveness of Vision Transformer (ViT) architectures for automated skin lesion classification using the HAM10000 dataset. Through a structured pipeline involving image normalization, augmentation, artifact removal, and metadata cleaning, we prepared a balanced dataset suitable for deep learning applications. The initial ViT model did not incorporate dropout regularization and showed signed of overfitting; however, after introducing drop-out in the final model, generalization performance significantly improved. The fine-turned ViT model ultimately achieved 99% training accuracy and approximately 90% testing accuracy, outperforming many traditional convolutional approaches in both precision and robustness. Beyond quantitative metrics, this research emphasized model fairness by analyzing metadata such as age and lesion site to ensure that demographic factors did not introduce bias in classification outcomes. The integration of strong predictive performance, regularization through dropout, and interpretability underscores the potential of ViT-based frameworks as reliable computer-aided diagnostic tools to assist dermatologists in early skin caner detection.

V. Future work

Future research can further enhance the model's performance and practical applicability through several directions:

- Model Enhancement: Integrate the techniques from *Skin-DeepNet* (Al-Waisy et al.) such as adaptive contrast enhancement (AGCWD), hybrid Mask R-CNN + GrabCut segmentation, and ensemble fusion to improve classification accuracy and lesion boundary precision.
- Dataset Expansion: Validate model robustness on larger and more diverse datasets such as ISIC 2019 and PH2.
- Explainability: Employ visualization tools like Grad-CAM and attention heatmaps to interpret ViT attention regions and improve clinical trust.
- Deployment Optimization: Develop lightweight, real-time versions for mobile or point-of-care diagnostic applications.
- Multimodal Integration**:** Combine clinical metadata (e.g., patient history, lesion evolution) with image-based learning to enhance diagnostic accuracy.

In summary, the proposed Vision Transformer framework establishes a solid foundation for intelligent skin cancer diagnosis. By incorporating advanced hybrid methods such as *Skin-DeepNet*, future iterations can further elevate testing accuracy and strengthen the role of AI in early melanoma detection and dermatological screening.

A. Tables

Table 3: training classification report

Class	Precision	Recall	F1-Score	Support
Akiec	0.94	0.99	0.96	250
Bcc	0.99	0.98	0.99	393
Bkl	1	0.96	0.98	841
Df	0.99	1	0.99	88
Mel	0.97	0.97	0.97	851
Nv	0.99	1	1	5129
Vasc	0.99	0.99	0.99	108
Overall Accuracy			0.99	7660
Macro Avg	0.98	0.99	0.98	7660
Weighted Avg	0.99	0.99	0.99	7660

Table 4: Testing Calssification Report

Class	Precision	Recall	F1-Score	Support
Akiec	0.70	0.90	0.79	49
Bcc	0.86	0.86	0.86	77
Bkl	0.92	0.75	0.83	165
Df	0.79	0.88	0.83	17
Mel	0.80	0.72	0.76	167
Nv	0.94	0.97	0.95	1006
Vasc	0.91	0.95	0.93	22
Overall Accuracy			0.91	1503
Macro Avg	0.85	0.86	0.85	1503
Weighted Avg	0.91	0.91	0.91	1503

References

The template will number citations consecutively within brackets [1]. The sentence punctuation follows the bracket [2]. Refer simply to the reference number, as in [3] do not use "Ref. [3]" or "reference [3]" except at the beginning of a sentence: "Reference [3] was the first ..."

Number footnotes separately in superscripts. Place the actual footnote at the bottom of the column in which it was cited. Do not put footnotes in the abstract or reference list. Use letters for table footnotes.

Unless there are six authors or more give all authors' names; do not use "et al.". Papers that have not been published, even if they have been submitted for publication, should be cited as "unpublished" [4]. Papers that have been accepted for publication should be cited as "in press" [5]. Capitalize only the first word in a paper title, except for proper nouns and element symbols.

For papers published in translation journals, please give the English citation first, followed by the original foreign-language citation [6].

[1] American Academy of Dermatology, “Skin cancer,” AAD, Jun. 20, 2025. [Online]. Available: https://www.aad.org/media/stats-skin-cancer

[2] ISIC Archive, “ISIC Challenge Datasets,” [Online]. Available: https://challenge.isic-archive.com/data/

[3] P. Tschandl, C. Rosendahl, and H. Kittler, “The HAM10000 dataset: A large collection of multi-source dermatoscopic images of common pigmented skin lesions,” Scientific Data, vol. 5, p. 180161, Aug. 2018.

[4] Skin Cancer Foundation, “Skin Cancer Facts & Statistics,” [Online]. Available: https://www.skincancer.org/skin-cancer-information/skin-cancer-facts/

[5] U. Bhimavarapu and G. Battineni, “Skin lesion analysis for melanoma detection using the novel deep learning model Fuzzy GC-SCNN,” Healthcare, vol. 10, no. 5, p. 962, May 2022.

[6] I. D. Mienye and T. G. Swart, “A comprehensive review of deep learning: Architectures, recent advances and applications,” Information, vol. 15, no. 12, p. 755, Nov. 2024.

[7] G. Alwakid, W. Gouda, M. Humayun, and N. Z. Jhanjhi, “Diagnosing melanomas in dermoscopy images using deep learning,” Diagnostics (Basel), vol. 13, no. 10, p. 1815, May 2023.

[8] “Recent advancements and perspectives in the diagnosis of skin diseases using machine learning and deep learning: A review,” 2024.

[9] L. Papa, P. Russo, I. Amerini, and L. Zhou, “A survey on efficient vision transformers: Algorithms, techniques, and performance benchmarking,” 2023.

[10] S. Remya, T. Anjali, and V. Sugumaran, “A novel transfer learning framework for multimodal skin lesion analysis,” IEEE Access, vol. 12, pp. 50738-50754, 2024.

[11] Y. Dahdouh, A. B. Anouar, and M. Ben Ahmed, “Embedded artificial intelligence system using deep learning and Raspberry Pi for the detection and classification of melanoma,” IAES Int. J. Artif. Intell., vol. 13, no. 1, pp. 1104-1111, 2024.

[12] F. Firdaus et al., “Segmentation of skin lesions using convolutional neural networks,” Comput. Eng. Appl. J., vol. 12, no. 1, pp. 58-67, 2023.

[13] S. Hamida, D. Lamrani, O. El Gannour, S. Saleh, and B. Cherradi, “Toward enhanced skin disease classification using a hybrid RF-DNN system leveraging data balancing and augmentation techniques,” Bull. Electr. Eng. Inf., vol. 13, no. 1, pp. 538–547, 2024.

[14] M. A. Khan, K. Muhammad, M. Sharif, T. Akram, and V. H. C. de Albuquerque, “Multi-class skin lesion detection and classification via teledermatology,” IEEE J. Biomed. Health Inform., vol. 25, no. 12, pp. 4267-4275, 2021.

[15] N. Gessert, M. Nielsen, M. Shaikh, R. Werner, and A. Schlaefer, “Skin lesion classification using ensembles of multi-resolution EfficientNets with metadata,” MethodsX, vol. 7, p. 100864, 2020.

[16] A. Esteva et al., “Dermatologist-level classification of skin cancer with deep neural networks,” Nature, vol. 542, no. 7639, pp. 115-118, 2017.

[17] Q. Liu, L. Yu, L. Luo, Q. Dou, and P. A. Heng, “Semi-supervised medical image classification with relation-driven self-ensembling model,” IEEE Trans. Med. Imaging, vol. 39, no. 12, pp. 3429-3440, 2020.

[18] A. Adealnabi, S. Eduardo J, M. Becevic, E. H. Smith, P Rao, “Transformers in Skin Lesion Classification and Diagnosis: A systematic Review, Health Informatics, September 2024.

[19] A. S. Al-Waisy, S. AlFahdawi, M.I. Khalaf, M. A. Mohmmed, B. All-Attar, M.N. AL-Andoli, “A Deep Learning Framework for Automated early Diagnosis and Classification of Skin Cancer Lesions in Dermoscopy Images”, Scientific Reports, vol. 15, no. 1, p.31234, August 2025.

[20] M. Jia, “Inside a Vision Transformer (ViT): How Image is Classified Step by Step,” *GoPenAI*, Jul. 3, 2025. [Online]. Available: https://blog.gopenai.com/inside-a-vision-transformer-vit-how-image-is-classified-step-by-step-0af45d5acbca. [Accessed: Nov. 08, 2025].

IEEE conference templates contain guidance text for composing and formatting conference papers. Please ensure that all template text is removed from your conference paper prior to submission to the conference. Failure to remove template text from your paper may result in your paper not being published.